

## MODELING OF ELECTRONIC SPECTRA OF IONIC FORMS OF EOSIN AND ERYTHROSIN

A. V. Rogova,<sup>1</sup> F. N. Tomilin,<sup>1,2</sup>  
M. A. Gerasimova,<sup>1</sup> and E. A. Slyusareva<sup>1</sup>

UDC 544.18, 544.17, 535.34, 535.37

*Multistage dissociation of fluorescein dyes, widely used in biological labeling, yields a variety of ionic and tautomeric forms in a wide range of pH values. In contrast to well-studied absorption spectra, the emission spectra are not quite readily interpreted due to their strong overlapping and proton transfer in electronically excited states. The least studied are the fluorescent properties of eosin and erythrosin dyes containing heavy atoms (Br, I), in which the characteristics of the dianionic form only are reliably determined. In the framework of the density functional theory using the B3LYP-functional including nonequilibrium solvation, the geometries of the series of ionic forms of eosin and erythrosin in the ground and excited states are found, and the electronic spectra are calculated. Based on the identified linear regression of the calculated and experimental data for the earlier resolved electronic spectra, for the first time, the emission spectrum maxima of the monoanionic, neutral quinoid, and cationic forms of the dyes are determined. The spectral peculiarities (Stokes shifts) are discussed in terms of variation of the molecule and ion geometries in the ground and excited states.*

**Keywords:** eosin, erythrosin, ionic forms, non-stationary density functional theory TD-DFT, B3LYP, polarized continuum model, electronic spectra, absorption, fluorescence.

### INTRODUCTION

Fluorescein and its halogen-substituted (Br, I) homologs (eosin, erythrosin) are used for biological labeling and visualization of colorless systems (cells, proteins, etc.) [1, 2] and as acceptors and converters of the electronic excitation energy [3, 4] due to their strong absorption in the visible spectrum and their fluorescent, phosphorescent, and photochemical properties. As a result of a three-stage dissociation in aqueous solutions, fluorescein dyes can exist in dianionic, monoanionic neutral, and cationic forms and can additionally have a number of tautomers of one and the same ionic state. In view of the fact that protonation/deprotonation frequently occurs in a chromophoric group, such changes most radically influence the absorption and emission spectra. In contrast to well-studied absorption spectra of ionic fluorescein dyes [5–7], the complex structure of the emission spectra in a wide pH range is not quite clear due to the variety of these forms, overlapping of broad spectra, and proton transfer in the electronically excited states [8]. The least studied dyes are those containing heavy atoms (eosin, erythrosin), whose neutral forms are poorly soluble and whose constants of the dianionic-monoanionic and monoanionic-neutral equilibrium are close [5].

One of the ways of studying the energy structure of molecules in the cases where the experimental investigations are difficult is a quantum-chemical calculation approach. The purpose of this work is to determine the geometry and spectral properties of a number of ionic and tautomeric forms of eosin and erythrosin. The results of

---

<sup>1</sup>Siberian Federal University, Krasnoyarsk, Russia, e-mail: arogova1927@gmail.com; felixnt@gmail.com; marina\_2506@mail.ru; ESlyusareva@sfu-kras.ru; <sup>2</sup>Kirenskiy Institute of Physics of the Siberian Branch of the Russian Academy of Sciences – Division of the Federal Research Center “Krasnoyarsk Scientific Center of the Siberian Branch of the Russian Academy of Sciences”, Krasnoyarsk, Russia. Translated from *Izvestiya Vysshikh Uchebnykh Zavedenii, Fizika*, No. 8, pp. 115–121, August, 2020. Original article submitted July 6, 2020.

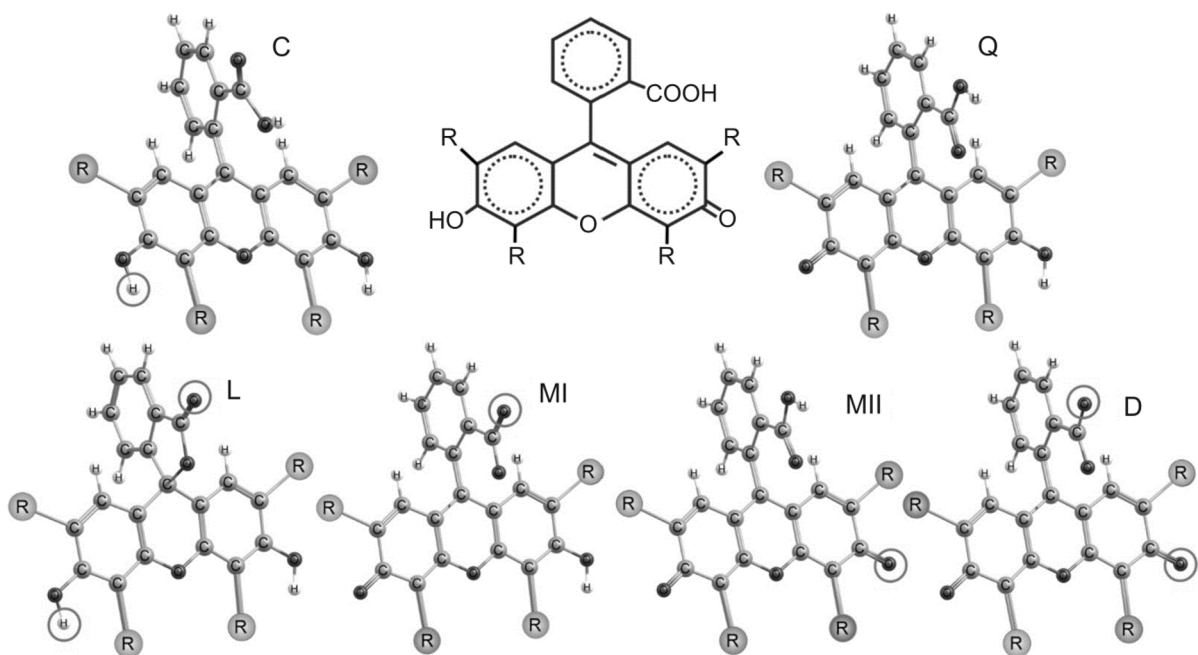


Fig. 1. Ionic and molecular forms of eosin ( $R = \text{Br}$ ) and erythrosin ( $R = \text{I}$ ): C – cation, Q – neutral quinoid, L – neutral lactone, MI – monoanion 1, MII – monoanion 2, D – dianion. Circles denote the fragments containing differences from the neutral quinoid form.

quantum-chemical calculations using the time-dependent density functional theory (TD-DFT) were compared with the experimental data obtained by the method of absorption and fluorescent spectroscopy in a wide range of pH values. An analysis of the linear regression parameters between the calculated and experimental values allowed us to predict for the first time the values of the fluorescence maxima of monoanionic, neutral, and cationic forms of eosin and erythrosin. A comparison of the spectral properties of the dyes differing in the halogens-substituents was performed from the viewpoint of the spatial structure of the molecules under excitation.

## METHODS

The atomic and electronic structure, the electron density distributions, the emission and absorption spectra, and the oscillator strengths for ionic and molecular forms of eosin and erythrosin, taking into account the solvent, were calculated using the density functional theory (DFT). The calculations were performed for dianionic, cationic, two tautomers of neutral (quinoid and lactone), and two tautomers of monoanionic forms of eosin and erythrosin (Fig. 1). For the fluorescein molecule [8, 9], which is the basic structure for the dyes under study, there is also a zwitterionic neutral form, but in the calculations of its halogen-substituted derivatives, we failed to identify its stable configuration. All calculations were performed using the B3LYP-functional [10, 11]. The ionic forms of eosin were calculated using the *aug-cc-PVDZ*-basis containing diffusion functions in addition to polarization functions. Due to the absence of its parametrization for iodine, for erythrosin, we used the *ADZP*-basis, in its characteristics closest to *aug-cc-PVDZ*. The absorption spectra for all ionic and molecular forms were obtained with the time-dependent (TD) theory [12, 13].

It was shown earlier [8, 9] that when the solvent is included into consideration, the best approach is to use the polarized continuum model (PCM) taking into account nonequilibrium solvation [14, 15]. Under stationary conditions, for the dielectric constant of the solvent, the values that depend on temperature and pressure only are used. Nevertheless, when studying dynamic processes, it is necessary to take into account the time of relaxation of the solvent polarization. Then at a characteristic time shorter than the time of relaxation of the solvent, there is a delay in the

solvent response. To describe this process, we can use the term of a “fast” dielectric constant that is in equilibrium with the dissolved substance, while the other component is “slow” compared to the variation of the electron density of the dissolved substance. This approach was termed as the TD-DFT calculation including nonequilibrium solvation into account [15]. For this geometry, the emission spectrum was obtained using TD-DFT. All calculations were performed in the GAMESS program [16].

When calculating the spectral characteristics, it is important to know whether the optical transitions are accompanied by a charge transfer, which in its turn influences the choice of a functional. A criterion for distinguishing the local transitions from the charge-transfer and Rydberg transitions is the analysis of the so-called  $\Lambda$ -parameter [17]. The local excitations ( $0.45 < \Lambda < 0.89$ ) are characterized by large overlapping of molecular orbitals. This indicates the similarity of the spatial regions of the occupied and virtual molecular orbitals of the molecule involved in the excitation. In our calculations, for all ionic forms the  $\Lambda$ -parameter was within the limit  $0.51 < \Lambda < 0.71$ , which suggests the absence of a significant role of charge transfer in absorption and emission.

## RESULTS AND DISCUSSION

### Absorption and emission spectra

In the processes of light absorption by the molecules of organic compounds, the primary role belongs to the difference in the energies of their highest occupied orbital (HOMO) and the lowest unoccupied molecular orbital (LUMO). It is this very transition that determines the long-wavelength absorption band. An important factor of the influence of the substituents on the electronic absorption spectrum and the probability of electronic transitions is the removal of the restriction on symmetry. An introduction of substituents in the general case removes the symmetry restriction and increases the intensity of light absorption, which is observed in the halogen-substitution of hydrogen for bromine and iodine in fluorescein dyes.

The calculated strengths of the transition oscillators in absorption supported the availability of strong bands in the visible spectrum for all ionic and molecular forms but for the lactonic form (Table 1). Note that the absorption spectrum of erythrosin is shifted towards the red region (by 2–27 nm for different forms) compared to that of eosin. There is a good correlation of the calculated transition energies in absorption with the energy of the respective position of the maxima of the electron-vibrational spectrum for both dyes (Figs. 2 and 3). In order to obtain a linear regression, we additionally used the experimentally available values of the peak emissions of the dianionic forms  $D^*$  of the dyes under study (536 nm for eosin and 547 nm for erythrosin) [6].

It is seen in Figs. 2 and 3 that the MII point lies close to the regression line – a sign that the MII-form is available in the solution, while the MI point falls out of the regression both for eosin and erythrosin. It was shown many times [5] that it is the MII monoanion dissociated to form a hydroxyl group (Fig. 1) which is realized in the experiment. The absorption wavelength for a neutral molecule presented by two tautomers Q and L, according to the calculations, corresponds to the quinoid form Q.

The characteristics for D-, MII-, Q- and C-forms, associated with the transition probability (absorption oscillator strength and molar extinction coefficient, Table 1), also have a high linear correlation  $R^2 = 0.96$ – $0.98$  for both dyes, which implies adequacy of the selected calculation procedures.

The linear regression obtained for the calculated and experimental transition energies for the D-,  $D^*$ -, MII-, Q- and C-forms can be used for predicting the fluorescence spectra of ionic and molecular forms, which cannot be determined experimentally. To do so, from the derived regression equations taking into account the calculated emission energies we determined the maximum values in the fluorescence spectra. For eosin and erythrosin, they were found to be 614 and 613 nm for the  $Q^*$ -form, 473 and 494 nm for the  $C^*$ -form, and 604 and 690 nm for the  $MII^*$ -form, respectively. The traces of these maxima can be followed in the complex fluorescence contours of the dyes in an acid media, which represent mixtures of different ionic and/or molecular forms (inserts in Figs. 2 and 3). The transitions with the shortest wavelengths correspond to the cationic  $C^*$ -form of the dyes and are not detected in the fluorescence spectra up to pH 0.5–0.6. According to [5], the cation-neutral equilibrium constants are found to be equal to  $-2$  for eosin and  $-2.4$  for erythrosin, which suggests existence of this form beyond the pH range of the solvent.

TABLE 1. Spectral Characteristics of Ionic and Molecular Forms of Eosin and Erythrosin in Water

Ionic forms	Absorption				Emission		Stokes shift
	Calculation		Experiment [5]		Calculation		Calculation
	$\lambda_{S_0 \rightarrow S_1}$ , nm	$f_{S_0 \rightarrow S_1}$	$\lambda^{\max}$ , nm	$\epsilon^{\max} \cdot 10^{-3}$ , L·mol <sup>-1</sup> ·cm <sup>-1</sup>	$\lambda_{S_1 \rightarrow S_0}$ , nm	$f_{S_1 \rightarrow S_0}$	$\tilde{\nu}$ , cm <sup>-1</sup>
Eosin							
D	493	1.20	515	96.7	510	1.17	710
MI	471	0.76	517–519	81.9	518	0.33	1930
MII	507	1.24			576	0.83	2340
L	288	0.11	480–485	8.5	295	0.07	770
Q	478	0.77			584	0.47	3820
C	442	0.89	453–455	44.5	461	0.80	950
Erythrosin							
D	498	1.21	525	94.6	522	1.13	920
MI	477	0.75	530	91.9	526	0.57	1930
MII	512	1.25			596	0.76	2740
L	296	0.09	500	11.4	298	0.07	260
Q	491	0.69			556	0.38	2370
C	469	0.82	462	45.2	487	0.70	810

Note.  $\lambda_{S_0 \rightarrow S_1}$  and  $f_{S_0 \rightarrow S_1}$  – are the absorption wavelength and the transition oscillator strength  $S_0 \rightarrow S_1$  (calculation),  $\lambda^{\max}$  and  $\epsilon^{\max}$  – is the wavelength of the absorption spectrum maximum and the molar extinction coefficient at this wavelength (experiment),  $\lambda_{S_1 \rightarrow S_0}$  and  $f_{S_1 \rightarrow S_0}$  – are the emission wavelength and the transition oscillator strength  $S_1 \rightarrow S_0$  (calculation).

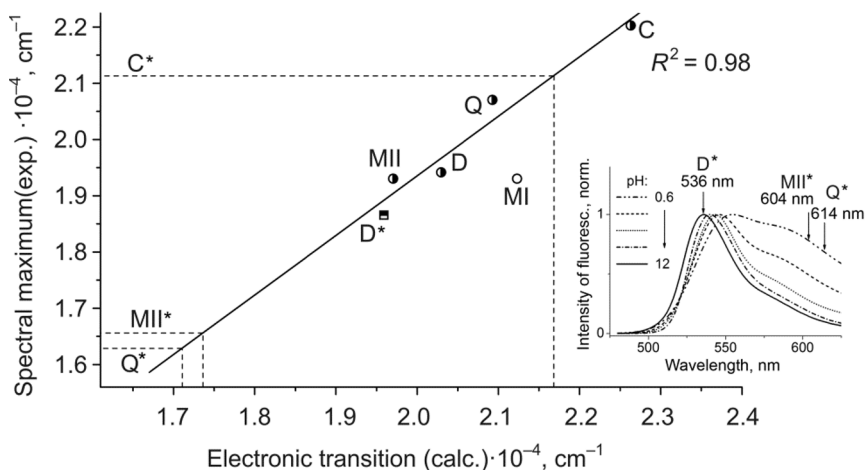


Fig. 2. Linear regression between the calculated and experimental wavelengths in the absorption spectra for D-, MII-, Q-, C-forms and the emission D\*-form of eosin. Theoretical predictions are shown for the cases where the experimental data are unavailable (emission of MII\*, Q\* and C\*-forms). Insert – positions of the dianionic maximum and the predicted MII\*- and Q\*-forms in the fluorescence spectra.

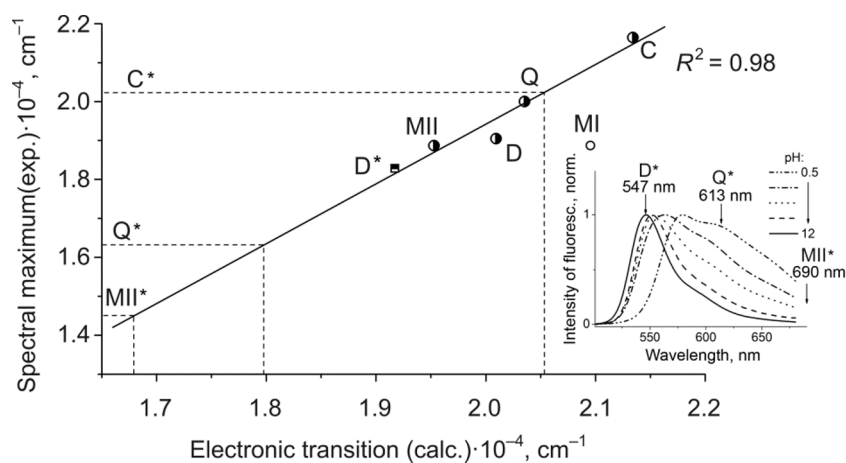


Fig. 3. Linear regression between the calculated and experimental wavelengths in the absorption spectra for the D-, MII-, Q-, C-forms and the emission D\*-form of erythrosine. Theoretical predictions are shown for the cases where the experimental data are unavailable (emission of MII\*, Q\* and C\*-forms). Insert – positions of the dianionic maximum and the predicted MII\*- and Q\*-forms in the fluorescence spectra.

Noteworthy is the high value of the Stokes shift for the monoanionic and neutral quinoid forms of the dye when the maximum value at  $3820\text{ cm}^{-1}$  (106 nm) for the eosin quinoid is reached. A large difference between the absorption and emission energies can be discussed in terms of the changed molecular geometry as a result of excitation and subsequent relaxation into an equilibrium excited state.

### Molecular orbitals and geometry of molecules in the ground and excited states

Figure 4 presents the geometry of the molecules in the ground state ( $S_0$ ) and HOMO-orbitals for this state; and the geometry of the molecules in the excited state ( $S_1^*$ ) and the respective LUMO molecular orbitals from which emission occurs. Since eosin and erythrosin have close molecular structure, their orbitals are also close in the shapes.

It is clear from Fig. 4 that the upper occupied molecular orbitals demonstrate  $\pi$ -bonding character for carbon atoms and non-bonding character for oxygen and halogen atoms. The lower unoccupied orbitals are also located on the tricycle and have a similar nature. For the dianion during a HOMO – LUMO transition there is no electron density transfer, hence no electron transfer processes are observed. In the ground  $S_0$ -state the MII monoanion and D dianion possess a high oscillator strength ( $> 1$ ), which also implies a local nature of the optical transitions and a potentially high quantum yield.

In all calculated structures, there is a perceptible difference in the geometries of the ground and excited states. In order to describe the changes in the molecule geometries under electronic excitation, we used a number of dihedral angles (Fig. 5). Angles  $\alpha_1$  and  $\alpha_2$  correspond to the in-plane bending of the 2–4 tricycle from the ground  $S_0$ - to the excited  $S_1^*$ -state of the dye. Angles  $\gamma_1$  and  $\gamma_2$  indicate the plane deflection of the 2–4 tricycle in states  $S_0$  or  $S_1^*$ , and angle  $\beta$  characterizes the plane change of ring 1 with respect to the 2–4 chromophoric tricycle in states  $S_0$  or  $S_1^*$ .

The largest differences in the molecule geometries in the ground and excited states are observed in the quinoid Q- and monoanionic MII-forms (Table 2). Upon relaxation of these forms, there is also a rotation of the carboxyl group relative to monocycle 1, and that of monocycle 1 relative to the tricycle. This is observed in a larger Stokes shift for these forms. To a lesser degree a change in the geometry during the transition into an excited state is manifested for cation C and monoanion MI, and even less so for dianion D (Table 2). For the lactonic form L, either for eosin and

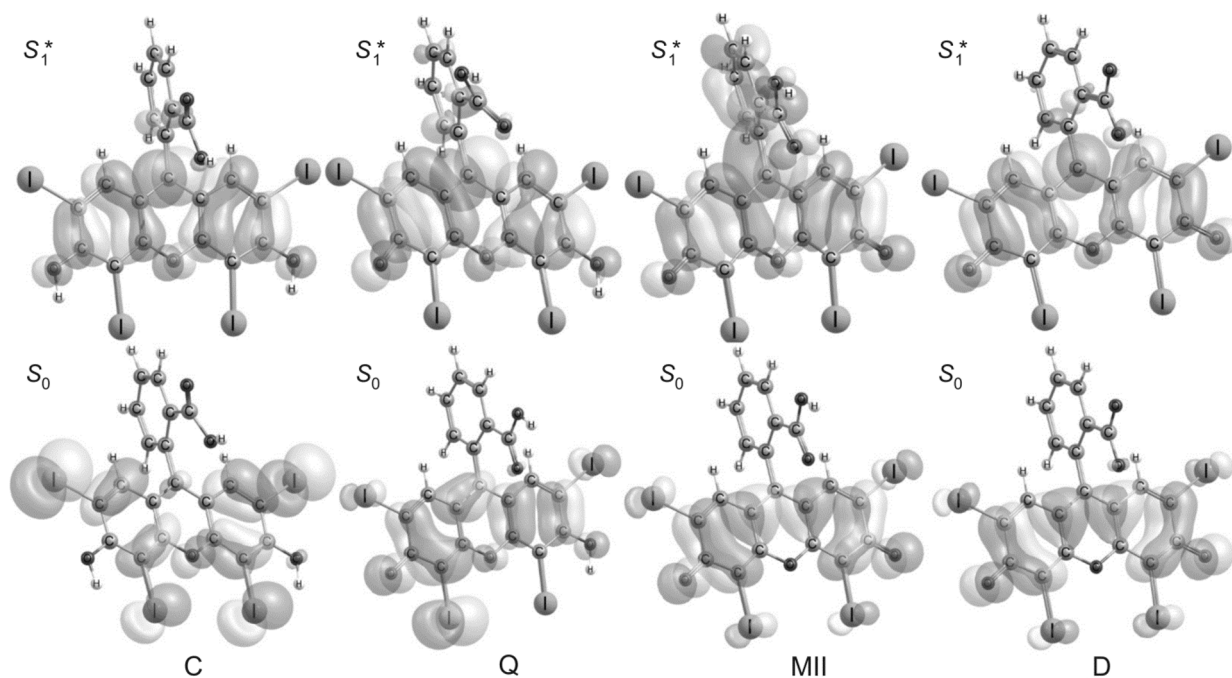


Fig. 4. Molecular orbitals for the ground  $S_0$ - and excited  $S_1^*$ -states of ionic forms of erythrosin.

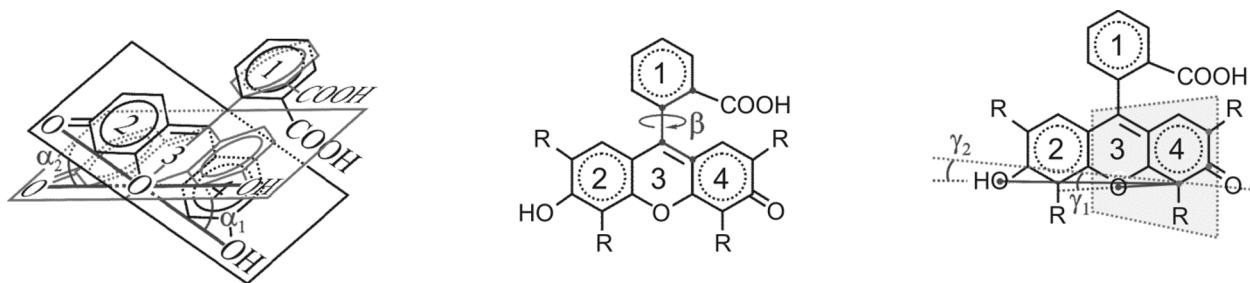


Fig. 5. Angles characterizing the change in the spatial structure of the dyes under excitation.

erythrosin, there are no cardinal geometry changes during their transition into excited states (Table 2); therefore, this form is characterized by a smaller Stokes shift.

A change of the tricycle plane for the quinoid form of eosin is characterized by  $\Delta\gamma_1 = 2.8^\circ$  and  $\Delta\gamma_2 = 3.3^\circ$ , while for erythrosin  $\Delta\gamma_1 = 0.3^\circ$  and  $\Delta\gamma_2 = 0.6^\circ$ . Comparatively heavy and sluggish iodine atoms favor weak conformation mobility of the chromophoric tricycle of erythrosine, which can serve as a reason for a small Stokes shift of erythrosin ( $2380\text{ cm}^{-1}$ ) compared to that of eosin ( $3800\text{ cm}^{-1}$ ).

## SUMMARY

The quantum-chemical calculations of the spectra of ionic and molecular forms of halogen-substituted fluorescein – eosin and erythrosin – have been performed using the time-dependent density functional theory. The calculation efficiency has been demonstrated by comparing the calculated transition energies in the absorption and the oscillator strengths with the experimentally measured absorption spectral peaks and the molar extinction coefficients of the dianionic, monoanionic, quinoid, and cationic forms. Using the linear regression found between the calculated and

TABLE 2. Changes in Geometry of Molecular Forms of Eosin and Erythrosin under Electronic Excitation (Calculation)

Angle, deg	D	MI	MII	Q	L	C
Eosin						
$\alpha_1$	0.9	0.7	5.7	4.1	0.2	2.6
$\alpha_2$	1.1	2.3	4.1	2.9	0.3	1.8
$\Delta\beta$	8.1	14.7	26.2	18.4	0.5	12.2
$\Delta\gamma_1$	0.2	0.5	2.6	2.8	1.5	1.4
$\Delta\gamma_2$	0.8	1.6	3.1	3.3	1.7	0.8
Erythrosin						
$\alpha_1$	1.4	0.67	6.9	5.2	0.3	0.5
$\alpha_2$	1.8	3.4	4.6	5.7	0.8	1.5
$\Delta\beta$	10.4	18.1	29.3	28.2	0.8	2.8
$\Delta\gamma_1$	0.8	0.3	1.9	0.3	1.6	0.5
$\Delta\gamma_2$	0.7	0.7	2.7	0.6	1.7	1.4

Note.  $\Delta\beta$ ,  $\Delta\gamma_1$  and  $\Delta\gamma_2$  indicate variations in the angles  $\beta$ ,  $\gamma_1$  and  $\gamma_2$ , respectively, during the transition of a dye from the ground to the excited state.

experimental data, for the first time the fluorescence peak positions have been predicted for the cationic (473 and 494 nm), monoanionic (604 and 690 nm), and neutral quinoid (614 and 613 nm) forms of eosin and erythrosin, respectively. It has been shown that despite the similar sets of ionic and molecular forms, the spectral properties of the experimental fluorescein dyes essentially depend on the type of halogen affecting the “stiffness” of the chromophoric tricycle.

This work was performed according to the State assignment of the RF Ministry of science and higher education (FSRZ-2020-0008) and was supported by funding from the RFBR, Project No. 19-02-00450.

## REFERENCES

1. A. M. El-Brashy, M. Metwally El-Sayed, and F. A. El-Sepai, *Il Farmaco*, **59**, 809 (2004).
2. D. Gao, Y. Tian, F. Liang, *et al.*, *J. Lumin.*, **127**, 515 (2007).
3. M. A. Gerasimova, A. G. Sizykh, and E. A. Slyusareva, *J. Photochem. Photobiol. B*, **97**, 117 (2009).
4. A. G. Sizykh, E. A. Tarakanova, and L. L. Tatarinova, *Quant. Electr.*, **30**, No. 1, 40 (2000).
5. N. O. Mchedlov-Petrosyan, *Vestnik of Kharkov Nat. Univ.*, No. 626, *Khimiya*, Iss. 11(34), 221 (2004).
6. E. A. Slyusareva and M. A. Gerasimova, *Russ. Phys. J.*, **56**, No. 12, 1370 (2014).
7. N. Klonis and W. H. Sawyer, *J. Fluoresc.*, **6**, 147 (1996).
8. M. A. Gerasimova, F. N. Tomilin, E.Yu. Malyar, *et al.*, *Dyes Pigm.*, **173**, 107851 (2020).
9. E. A. Slyusareva, F. N. Tomilin, A. G. Sizykh, *et al.*, *Opt. Spectrosc.*, **112**, No. 5, 729 (2012).
10. A. D. J. Becke, *J. Chem. Phys.*, **98**, 5648 (1993).
11. R. G. Yang and C. Lee, *Phys. Rev.*, **37**, 785 (1988).
12. E. K. Gross and W. Kohn, *Adv. Quantum Chem.*, **21**, 255 (1990).
13. M. E. Casida, *Recent Advances in Density Functional Materials, Part I* (Ed. D. P. Chong), World Scientific, Singapore (1995).
14. J. Tomasi, B. Mennucci, and R. Cammi, *Chem. Rev.*, **105**, 2999 (2005).
15. M. Cossi and V. Barone, *J. Chem. Phys.*, **115**, 4708 (2001).
16. M. W. Schmidt, K. K. Baldridge, J. A. Boatz, *et al.*, *J. Comput. Chem.*, **14**, 1347 (1993).
17. M. J. G.Peach, P. Benfield, T. Helgaker, *et al.*, *J. Chem. Phys.*, **128**, 044118 (2008).